IOP Publishing Journal of Physics D: Applied Physics
J. Phys. D: Appl. Phys. **48** (2015) 245202 (8pp) doi:10.1088/0022-3727/48/24/245202

Atmospheric pressure arc discharge with ablating graphite anode

V A Nemchinsky[1] and Y Raitses[2]

[1] Keiser University, Fort Lauderdale Campus, FL, 33309, USA
[2] Princeton Plasma Physics Laboratory, Princeton, NJ 08543, USA

E-mail: Vnemchinsky@keiseruniversity.edu

Received 8 January 2015, revised 23 April 2015
Accepted for publication 28 April 2015
Published 18 May 2015

Abstract

The anodic carbon arc discharge is used to produce carbon nanoparticles. Recent experiments with the carbon arc at atmospheric pressure helium demonstrated the enhanced ablation rate for narrow graphite anodes resulting in high deposition rates of carbonaceous products on the copper cathode (Fetterman *et al* 2008 *Carbon* **46** 1322–6). The proposed model explains these results with interconnected steady-state models of the cathode and the anode processes. When considering cathode functioning, the model predicts circulation of the particles in the near-cathode region: evaporation of the cathode material, ionization of evaporated atoms and molecules in the near-cathode plasma, return of the resulting ions to the cathode, surface recombination of ions and electrons followed again by cathode evaporation etc. In the case of the low anode ablation rate, the ion acceleration in the cathode sheath provides the major cathode heating mechanism. In the case of an intensive anode ablation, an additional cathode heating is due to latent fusion heat of the atomic species evaporated from the anode and depositing at the cathode. Using the experimental arc voltage as the only input discharge parameter, the model allows us to calculate the anode ablation rate. A comparison of the results of calculations with the available experimental data shows reasonable agreement.

Keywords: arc, electrodes, ablation, nanoparticles

(Some figures may appear in colour only in the online journal)

1. Introduction

An arc discharge with carbon electrodes is one of the promising methods to produce nanoparticles. In one embodiment of this methods, the arc is struck between a copper cathode and a graphite anode, see, for example [1, 2] and references therein. Experiments [3] showed that just after the ignition, the arc is in the cathode spot (CS) mode which is similar to a typical vacuum arc mode: a strong erosion of the cathode inside tiny cathode spots provides the atomic species ionized in the near-cathode region. In addition to a high cathode erosion, this mode is characterized by a complex electron emission mechanism [4]. After a short period of time ~1–10 s, the anode is heated up by plasma to temperatures high enough to cause the ablation of the anode material. As a result, the cathode becomes covered with products of the anode ablation and the arc turns into another mode—the anode ablation mode (AAM). The cathode in this mode does not melt or erode. On the contrary, the thickness of the graphite layer that covers the cathode, is either stabilized or increased in time [5].

Experiments with carbon arc at the atmospheric pressure of helium [1, 2] revealed that, depending on the diameter of the anode, the anode ablation rate changes dramatically from a very low rate for the wide anode to a high ablation rate for the narrow anode. For example, for the arc currents of 50 and 70 A and the inter-electrode gap of 2 mm, the high ablation rate mode was obtained with the anode diameter of smaller than 7–8 mm. The nature of this transformation is of a definite interest. This is because the abrupt increase of the anode ablation rate with the reduction of the anode diameter supersedes the expected increase of the current density at the anode. It is not clear if this ablation rate change represents different mechanisms of the arc operation or it could be explained in a framework of the same arc operation mechanism The goal of this paper is to explain this interesting behavior.

Modelling of the carbon arc discharge under conditions similar to that of [1, 2] was reported elsewhere [6, 7]. In [6], the heat and mass transfer in the gap between arc electrodes and outside the electrodes were simulated. Simulations predicted that the plasma velocity in the gap is very low (not exceeding 10 cm s^{-1}). This result was in an agreement with experimental results of [6]. Moreover, simulations predicted the arc plasma temperature of about 6500 K and the cathode temperature of about 1500 K. This cathode temperature is too low to provide necessary electron emission to support a typical arc current density at any reasonable cathode work function. The predicted anode temperature was rather high, about 3700 K [6].

In [7], the model predicted the ion current constitutes 80–90% of the total arc current (~10's A) at the cathode. This seems to be too high for a typical arc discharge. Indeed, it is not clear how the emitted electrons (10 to 20% of the total current) could have enough energy to generate such a high ion current to the cathode.

Concluding this brief review of the existing carbon arc models, it should be mentioned that modeling of the inter-electrode plasma is a very difficult task. With a relatively short inter-electrode gap (~a couple of millimeters [1]) and the low plasma temperature (~6500 K [6]), plasma could be far from the chemical and the thermal equilibriums. In this paper, we present a simplified steady-state arc model with a minimum of *a priori* assumptions. For the sake of this simplified analysis, we shall avoid detail considerations of the inter-electrode plasma. Moreover, being a steady-state one, the proposed model does not describe the initial stage of the arc development as well as possible arc instabilities.

This paper is organized as follows. The model of the cathode processes is described in section 2. The model of the anode thermal mode is suggested in section 3. The cathode model of section 2, and the anode model of section 3, are combined in section 4 to calculate the main characteristics of the arc. Section 5 summarizes the results.

2. The cathode processes model

While analyzing the cathode processes in the arc, the mechanism of the electron emission should be determined first. For carbon arc discharge, this problem was discussed in [3, 7–9]. In these works, it was postulated that the electron emission mechanism is the thermofield one. This conclusion goes along with experimentally measured cathode surface temperatures of above 3000 K [8].[1]

In the considered type of the arc discharge with the strong anode ablation, the cathode could be heated by two major mechanisms: a) bombardment by the ions generated in the near-cathode plasma (standard mechanism for the high pressure arcs) or b) by the particles evaporated from the anode that brought their latent heat of evaporation to the cathode. The second possibility was considered in [2, 9]. In particular, it was shown that in the case of a strong anode ablation, this mechanism is sufficient to heat the cathode up to the temperatures necessary to provide high enough thermionic electron emission [2]. However, in the case of the low anode ablation, this mechanism is not sufficient to heat the cathode to high temperatures necessary for sustaining the arc current by thermionic emission. Therefore, at least in the case of the wide anode (low ablation rate), the model should incorporate the standard way of the cathode heating by the ions.

[1] This temperature contradicts 1500 K obtained in [6]. Possible explanation of this discrepancy is that the temperature of the cathode surface in [6] was obtained by the extrapolation of the readings of the thermocouples mounted in the bulk of the cathode. Existence of the graphite deposits of an unknown thermal conductivity at the cathode surface could make this extrapolation questionable.

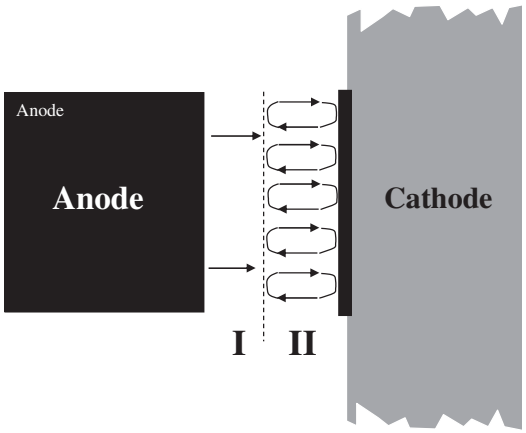

Figure 1. Schematic of inter-electrode plasma. Region I is the near-anode region and arc column. Region II is the near-cathode region with trapped ions.

2.1. Low anode ablation case (wide anode)

We shall start from the low ablation case at a steady-state. In conventional high-pressure thermionic arcs, the ions bombarding the cathode are resulted from the ionization of the working gas. In the considered carbon arc, the arc chamber is filled with a helium gas at the atmospheric pressure. The ionization potential of helium is so high and the plasma temperature is so low that one can neglect ionization of this so-called buffer gas. (The situation is different from that in welding arcs where both gases (argon and vapor from the electrodes) are in ionized state [10]). Therefore, the main source of the ions is ionization of carbon atoms and molecules evaporated from the carbonaceous cathode deposit. The carbon ions return to the cathode under influence of the electric field in the near-cathode sheath. At the cathode, these ions recombine with cathode electrons forming the cathode deposit. The deposit evaporates supplying atoms and molecules and so on. Thus, the particles are trapped between the cathode and the plasma in the near-cathode sheath.

The above process of particles circulation is similar to that considered in [11] for the case of a high-pressure arc with a refractory cathode. It was shown there that a very small amount of particles can escape from this trap. These escaped particles constitute the cathode erosion. In the carbon arc case, the cathode experiences the 'negative' cathode erosion due

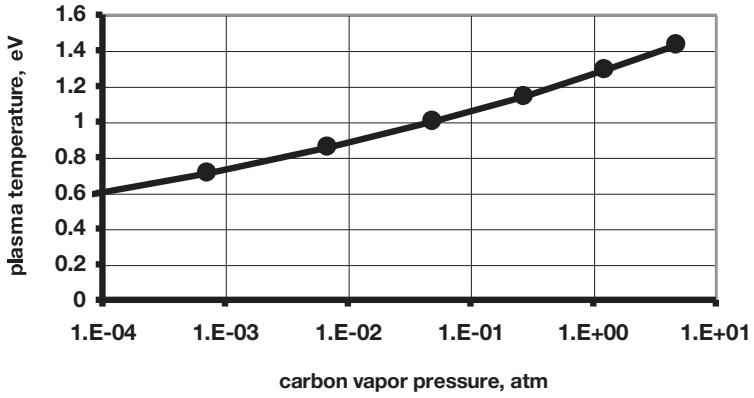

Figure 2. Plasma temperature of the carbon plasma that provides the maximum ion current density at a cathode.

to, a flow of carbon particles from the anode to the cathode. Therefore, for ions to leave this near cathode trap, they should move not only against the electric field but also against the gasdynamic flow of carbon atomic species from the anode. Assuming that particles can not escape from the trap, the pressure in the trap can be determined by the saturation pressure of carbon atoms and molecules $p(T_c)$ at the cathode temperature T_c. Note, that because particles evaporate and condense on the deposit with the same rate, there is no contribution of the latent heat to the cathode energy balance. This situation is shown schematically in figure 1.

The ion current density at the cathode surface is determined by the degree of ionization of vaporized particles. Without going into details of the ionization process, one can estimate the degree of ionization in the arc. From the existing model of the high-pressure arc (see, for example, [12], it follows that the parameters of the near-cathode plasma are such that the plasma provides the highest possible ion current density. This condition can be fulfilled at a certain plasma temperature. Figure 2 shows the predicted dependence of this temperature on the carbon vapor pressure. Although the plasma could be far from the ionization equilibrium, note that a) use of the Saha formula to calculate temperature at a given electron density (not vice versa!) doesn't lead to large error in plasma temperature T_p, and b) our calculations are not too sensitive to the T_p value. One can have reasonable results even setting $T_p = 0$.

Let us consider the cathode heat balance. The heat flux density at the cathode is

$$q = j_i(V_c + U_{ion} - \phi + 2T_p + H) - \frac{g_c(T_c)}{M}H - j_e\phi. \quad (1)$$

In (1), $V_c + 2T_p$ is the kinetic energy of the ion, $U_{ion} - \phi$ is the energy of the surface neutralization of the ion, and H is the latent heat of evaporation. Here: j_i and j_e are the ion and the electron current densities, respectively, V_c is the voltage drop in the cathode sheath, U_{ion} is the ionization potential, ϕ is the effective cathode work function, T_p is the plasma temperature, $g_c(T_c)$ is the net flux density ($\mathrm{kg\,m^{-2}\,s^{-1}}$) of the evaporated atoms, and M is the atom mass.

If all the evaporated atoms return back to the cathode, the net flux g_s turns to zero. This simplifies equation (1) to

$$q = j_i(V_c + U_{ion} - \phi + 2T_p) - j_e\phi. \quad (2)$$

The ion current density corresponds to the flux density of the evaporating particles,

$$j_i = \frac{\mathrm{ep}(T_c)}{\sqrt{2\pi MkT_c}}. \quad (3)$$

From the energy balance in the near-cathode plasma it follows that:

$$j_e V_c = j_i U_{ion} + 3.2kT_p(j_i + j_e). \quad (4)$$

Equation (4) implies that the emitted electrons are accelerated inside the cathode sheath and ionize the atoms of the working gas near the cathode (the first term in the RHS of equation (4)). The remaining heat is removed by the electrons flow deep inside the inter-electrode plasma (last term in the RHS of equation (4)).

Density of the electron emission is described by the Richardson–Dushman equation with the Schottky correction:

$$j_e = AT_c^2 \exp\left(-\frac{\phi}{kT_E}\right), \quad (5)$$

where ϕ is the effective cathode work function.

We considered the cathode arc attachment as a circle with R_c radius so that

$$I = \pi R_c^2(j_i + j_e), \quad (6)$$

where I is the arc current. The above equations should be amended by the equation of the heat balance at the cathode.

2.2. Approximate model of the cathode heat balance

In experiments [1, 2], the cathode was made of a thick copper disk of a few centimeters diameter. Keeping in mind that the cathode arc attachment does not exceed a few millimeters in diameter, the cathode body could be considered as infinite. Note, however, that arc does not contact the copper cathode because it is covered with a carbon deposit. The thickness of the deposit, L, depends on the duration of the arc and a mode of the arc operation. For example, after a couple of minutes of the arc operation, it is less than one millimeter thick for

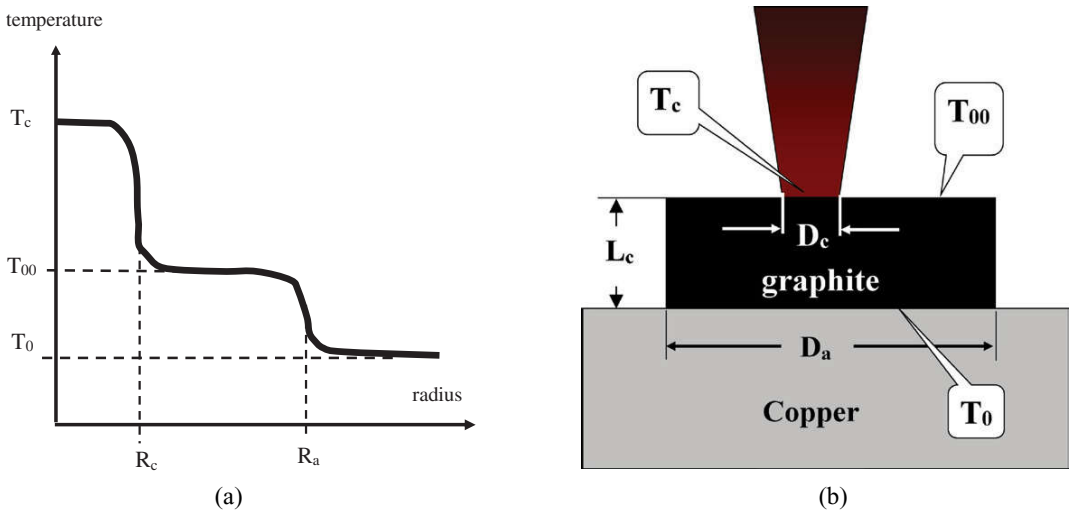

Figure 3. (a) Schematic of the temperature distribution at the cathode surface. R_c is the cathode attachment radius, R_a is the anode rod radius. T_0 is temperature of the copper-deposits boundary. T_{00} is the temperature created by the particles ablated from the anode at the cathode surface (background temperature). (b) Schematic view of the copper cathode, graphite deposits, and the near-cathode plasma.

the wide anode, and several millimeters thick for the narrow anode. If the thickness of deposits L is much larger than radius of the cathode attachment R_c, the deposit can be considered as an infinite medium. In this case, the cathode temperature at the cathode attachment due to the plasma heating power, $Q_c = \pi R_c^2 q$, is

$$T_c - T_0 = \frac{Q_c}{4\kappa R_c}, \tag{7a}$$

where κ is thermal conductivity of the graphite deposits, and T_0 is temperature far away from the attachment.[2] When the thickness of the deposits is much smaller than the attachment size $L << R_c$, the relationship between T_c and Q_c is different

$$T_c - T_0 = \frac{Q_c L}{\kappa \pi R_c^2}. \tag{7b}$$

Interpolation between both extreme cases, gives the following approximation:

$$T_c - T_0 = \frac{Q_c}{4\kappa R_c\left(1 + \frac{\pi R_c}{4L}\right)} \tag{7c}$$

Here, the temperature, T_0, is the temperature at the deposit-copper boundary. According to [13], the copper under the deposit is at the temperature below the copper melting point. For our simulations, we used $T_0 = 500$ K. It was found that the results of simulations are not sensitive to the value of T_0.

In the case of the low anode ablation and with the given I and L, the above equations allow one to obtain the cathode voltage fall and the cathode spot parameters, namely R_c, V_c, and T_p

[2] The coefficient γ in formula $Q_c = \gamma\kappa R_c(T_c - T_0)$ depends on the heat flux distribution inside the cathode attachment. For heat uniformly distributed inside the circle $\gamma = \pi$ and T_c is the maximum temperature. For temperature uniformly distributed $\gamma = 4$ and Q_c is the total heating power.

2.3. Cathode parameters in the case of strong anode ablation

We shall now modify the formulae of the previous sub-section in order to take into account the effect of carbon particles from the anode depositing on the cathode. First, note that particles are depositing at that portion of the cathode surface which faces the anode, i.e. at the circle at least of $R_a = 3$ mm radius. We assume (and our calculations and experiments confirm this) that the cathode area occupied by the deposit is larger than the area of the arc attachment to the cathode. This assumption implies that the heat flux of the depositing particles creates the background temperature of the cathode, T_{00}. Therefore, the temperature T_0, should be substituted with this elevated background temperature. The temperature distribution at the cathode surface is illustrated in figures 3(a) and (b).

Since thickness of the deposited layer L is smaller than the anode radius, the temperature, T_{00}, can be written as

$$T_{00} = \frac{Q_{c,a} L}{\kappa \pi R_a^2} + T_0. \tag{8}$$

Here, $Q_{c,a}$ is the net heat flux at the cathode surface created by the anode particles,

$$Q_{c,a} = \frac{HG_a}{M} f - \frac{\pi R_a^2 Hp(T_{00})}{\sqrt{2\pi MkT_{00}}}. \tag{9}$$

In equation (9), the first term is the heat of vaporization of the depositing particles. The second term counts for the power loosing by the deposited layer due to its own evaporation (not only within the cathode spot which is small compared to the whole circle of Ra radius!). Here G_a the anode ablation rate (kg s^{-1}). Coefficient f takes into account that only 60–70% of all the atoms evaporated from the anode is deposited at the cathode [2]. Using equations (8) and (9) for given $Q_{c,a}$ and L, it is possible to relate heat flux to the cathode, Q_c, and the temperature at the cathode that it creates. To do so, T_0 in

equation (7) should be substituted by T_{00} from equations (8) and (9).

The above formulae describe a procedure which allows us to calculate all characteristics of the current attachment at the cathode. For a given cathode geometry, the only input parameter that necessary for this procedure is the deposition rate on the cathode, fG_a,. Moreover, this procedure gives the cathode voltage drop V_c, which is used as the input parameter for modeling of the anode processes described below.

3. Anode processes model

3.1. Volt equivalent of the heat flux to the anode

Analysis of the anode heating processes is hampered by their multiplicity and lack of knowledge of the plasma properties and composition. To simplify the analysis we used the concept of so-called volt equivalent of the heat flux to the anode, V_{eq}. This concept is widely used in the analysis of high-pressure high-current arcs [14].

For short arcs, the total arc power IV_{arc} could be split into the power delivered to the cathode $I(V_c - \phi)$ and the power delivered to the anode $I(V_a + \phi)$. (It is suggested that the anode and cathode materials have the same work functions). Then, using voltages instead of powers, one can write

$$V_{eq} = V_{arc} - V_c + \phi \tag{10}$$

Here, the volt equivalent of the heat flux to the anode is defined as the ratio of the total heat flux to the anode to the arc current. It is important to note that, whereas V_c represents the actual cathode voltage, the V_{eq} is not directly related to the anode voltage. This is because in addition to the anode voltage drop, the volt equivalent includes also contributions to the anode heat balance due to the kinetic energy of the electrons impinging the anode, βT, per each electron entering the anode, and from neutralization of these electrons at the anode surface (the anode work function). The coefficient β depends on the electron distribution function and can be between 2.5–3.2 depending on the electron scattering mechanism. Other mechanism contributing to the heat balance at the anode are the radiation from the plasma (could important effect in high-current high-pressure arcs), and the anode voltage only if V_a positive.

The volt equivalent can be determined from the energy conservation law, equation (10). Then, using the experimental value of the arc voltage and the cathode voltage drop obtained in the previous section, it is possible to obtain the plasma heat flux to the anode.

3.2. Heat balance at the anode

We assume that the circular end of the anode facing the cathode is uniformly heated by the plasma fully covering the anode surface by the plasma. Also, it is assumed that there is no heat flux at the side of the anode. This implies the anode cooling by convection is neglected. These assumptions allow us to use 1D approximation and solve an algebraic equation instead of a two-dimensional differential equation.

The anode is heated by the arc, and is cooled by thermal conduction, radiation, and evaporation. Therefore, the heat balance at the anode is given by

$$IV_{eq} = S\left[\kappa\frac{\Delta T}{L_a} + \varepsilon\sigma_{SB}T_a^4 + (1-\eta)\frac{Hp(T_a)}{\sqrt{2\pi MkT_a}}\right], \tag{11}$$

where $S = \pi R_a^2$ is the anode area, ε is the graphite emissivity, σ_{SB} is the Stephan–Boltzmann constant, $p(T_a)$ is the graphite's density of the saturated vapor at the anode temperature T_a, k is the Boltzmann constant, M is the mass of the carbon atom, and H is the latent heat of evaporation. It is assumed that at the distance L_a from the anode surface, the temperature is kept at the room temperature T_{room} so that $\Delta T = T_a - T_{room}$. Here, the emissivity of graphite material is very close to unity [15]. Therefore, for the calculations presented in this paper, we used $\varepsilon = 1$.

In equation (11), the parameter η is the fraction of the evaporated atoms, which return back to the anode after experiencing a few collisions inside a layer of a few free paths thickness (the Knudsen layer) near the electrode. It has been shown that depending on arc conditions (plasma speed at the exit of the Knudsen layer), the return coefficient η could vary from ~18% (evaporation in vacuum [16]) to almost 100% that is typical for the welding arcs when vapor pressure of the eroding electrode is much lower than the ambient gas pressure [17–20].

In the above case of the evaporating cathode deposit, the evaporated atoms are almost all return back to the cathode. This is due to a high temperature of the cathode and a strong electric field in the near-cathode sheath directed to the cathode. In addition, the plasma flow from the anode to the cathode creates an additional drag force pushing atoms evaporated from the cathode back to the cathode. Parametric studies using different return coefficients demonstrated that the ablation rate depends very weakly on the η value. For example, for a 6 mm diameter anode, the ablation rate changes from 9.0 to 8.5 mg s^{-1} as η changes from zero to 0.8. Therefore, for all our following calculations, the parameter η was set to zero.

4. Modeling results

4.1. Solution method

Simulations were performed for experimental conditions reported in [1, 2]: the 65 A arc current, anode diameters from 6 to 12 mm. In order to minimize the influence of the power dissipated inside the inter-electrode gap, we used the arc voltage V_{arc} measured for the short interelectrode gap (one millimeter [1]).

For these simulations, the saturated vapor pressure at high temperatures $p(T)$ was taken from the [21] which is close to the data from [22]. The exact value of the graphite thermal conductivity, κ, at high temperatures is not well known. According to [23], the graphite thermal conductivity is 0.4 W cm^{-1} K^{-1} at temperature 2500 K. With a typically lower density than graphite, cathode carbon deposit has much lower thermal conductivity than graphite. For example, estimation

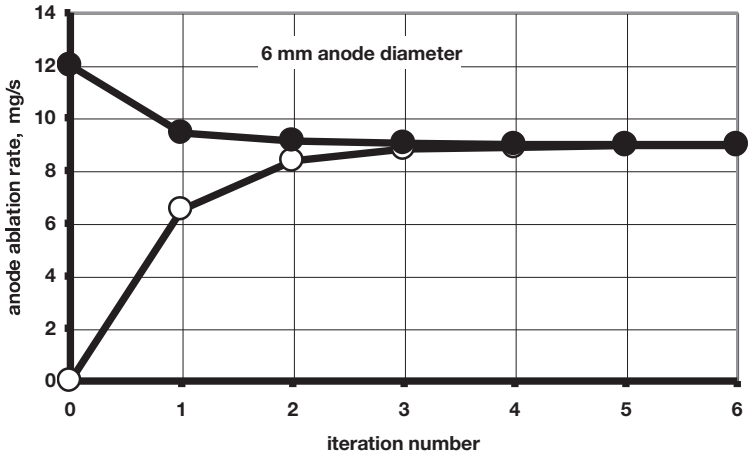

Figure 4. Anode ablation rate during the iteration process with high (black circles) and zero (white circles) initially picked ablation rates. (6 mm anode).

of the thermal conductivity of arc deposit measurements in [13] gives $\kappa \sim 0.01\,\mathrm{W\,cm^{-1}\,K^{-1}}$. Parametric calculations of the cathode characteristics at different values of the graphite thermal conductivities were performed in the range from 0.05 to $0.5\,\mathrm{W\,cm^{-1}K^{-1}}$. The calculations showed that the cathode voltage drop comparable with the measured voltage drop, can be obtained for $\kappa \sim 0.05 - 0.2\ \mathrm{W\,cm^{-1}K^{-1}}$. For simulations presented in this paper, we used $k = 0.1\,\mathrm{W\,cm^{-1}\,K^{-1}}$.

The following method of iterations was applied in these simulations:

Step 1. An arbitral value of the anode ablation rate, for example, from experimental results of [1, 2], was selected.

Step 2. With this ablation rate, the cathode attachment parameters were calculated according to the formulae of section 2.

Step 2.1 Pick some cathode temperature $T_c^{(0)}$

Step 2.2 Find the plasma pressure $p(T_c^{(0)})$

Step 2.3 Calculate ion current density according (3)

Step 2.4 Calculate electron current density according (5)

Step 2.5 Find cathode voltage drop V_c from (4)

Step 2.6 Find cathode attachment radius from (6)

Step 2.7 Calculate heat flux density at the cathode according to (2)

Step 2.8. Find new cathode temperature $T_c^{(1)}$.

Step 2.9 Adjust initially picked temperature $T_c^{(0)}$ to satisfy condition $T_c^{(0)} = T_c^{(1)}$

Step 3. Using equation (10), the volt equivalent of the heat flux to the anode was calculated

Step 4. Using this V_{eq} value, the anode temperature and erosion rate were calculated according to the formulae of section 3. Then, the anode ablation rate G_a was determined.

Step 5. The new ablation rate was used in Step 2.

Steps 2 to 5 were repeated until the model results converge. Figure 4 shows that the ablation rate converges very rapidly regardless of the initially picked ablation rate value.

4.2. Results of modeling

Table 1 shows calculated and measured results of following electrode characteristics for the 6 mm diameter anode (narrow anode) and the 12 mm diameter anode (wide anode). For the 6 mm anode, the calculated cathode current density is $570\,\mathrm{A\,cm^{-2}}$. Experiments with a sectioned cathode [13] established $230\,\mathrm{A\,cm^{-2}}$ as the lower current density limit.

Table 1. Electrodes parameters: anode diameter, volt equivalent of the anode heat flux, anode temperature, anode ablation rate, current density at the cathode, cathode voltage drop, cathode attachment temperature.

D_a (mm)	V_{eq} (V)	T_a (K)	G_a ($\mathrm{mg\,s^{-1}}$)	J_c ($\mathrm{A\,cm^{-2}}$)	V_c (V)	T_c (K)
6	10.7	3310	9.0	570	8.3	3260
12	7.2	2900	0.6	980	10.6	3350

Table 2. Fraction of different mechanisms in the total anode cooling.

D_a (mm)	Radiation	Evaporation	Thermal conduction
6	0.22	0.75	0.03
12	0.78	0.08	0.14

Measurements of the cathode temperature with IR camera gave $(3500 \pm 200)\,\mathrm{K}$ for 12 mm anode [13] that is comparable with the calculated temperature, 3350 K (table 1).

Table 2 compares contributions of different anode cooling mechanisms to the heat balance at the anode. Two main cooling mechanisms are radiation and evaporation: Evaporation is the main cooling mechanism for 6 mm diameter anode, while for 12 mm anode, cooling is mainly by radiation. Apparently, the thermal conduction is not so important especially in the case of the strong ablation.

The anode ablation rate is an important characteristic of the carbon arc discharge with consumed anode. In [1], the ablation rate was measured as the rate of the anode shortening ($\mathrm{mm\,s^{-1}}$). Ablation rate obtained here in gram per second, G_a, can be presented in the same units as $G_a/(\rho A)$, where $\rho = 2.27\,\mathrm{g\,cm^{-3}}$ is the graphite density and A is the anode surface area. Figure 5 compares the calculated and measured ablation rates [2]. Keeping in mind an approximate character of our

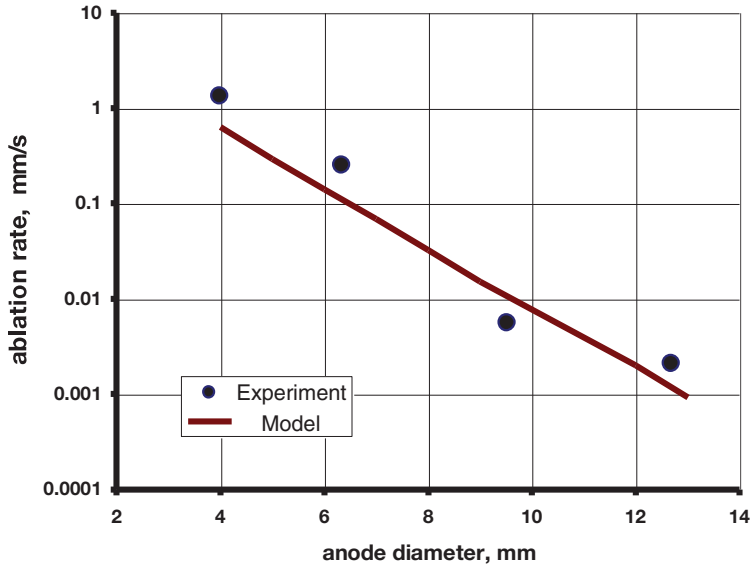

Figure 5. Anode ablation rate at different anode diameters. Points: experimental data [1].

calculations and lack of reliable data on material properties of graphite and cathode deposit at high temperature, the obtained agreement can be considered as satisfactory.

5. Conclusions

We developed a steady-state model of the carbon arc with ablating anode and compare modeling results of modeling with available experimental data. It is suggested that the atoms evaporated from the cathode are ionized and return back to the cathode in the form of ions. As a result, the circulation of atomic species in the near-cathode plasma is established. This circulation converts the energy of the emitted electrons, accelerated inside the cathode sheath to the plasma, into the ion heat flux to the cathode. This cathode heating is the major heating mechanism relevant to the arc regime with low anode ablation rates.

In the arc operation with high anode ablation rates, the latent heat carried by atoms and ions from the plasma to the cathode is one of the main cathode heating sources. This result is consistent with recent predictions of [2, 9].

2. The heat balance at the anode is considered. The anode is heated by the heat flux from plasma. The main mechanisms that cool the anode are radiation, evaporation and thermal conduction inside the anode body. To evaluate the heat flux from the plasma to the anode, the concept of the volt equivalent of the heat flux was used. The volt equivalent was obtained by using results of our cathode modeling (cathode voltage) and the experimental data on the arc voltage.

The presented model describes the large difference in the ablation rate for narrow and wide anodes observed in experiments. A comparison of the calculated and measured anode ablation rates shows a good agreement.

Several important issues of the energy balance at the electrodes remain outside the scope of this paper, but need to be addressed in the future works. For example, it is not clear what drives the electric current in the inter-electrode gap, electrical field or diffusion? In the former case, the anode voltage drop in the sheath is positive, i.e. electron attractive, while in the second case, it is negative, i.e. electron repelling. The heat flux to the anode can be strongly affected by the sign of the anode voltage drop. In the present work, we used the total arc voltage and therefore, did not address this issue. Moreover, the inter-electrode plasma effects should be also taken into consideration for a more detail and self-consistent modeling. Also, 2D effects due to the arc configuration, heat convection, and electrode geometry require 2D modeling of the arc discharge.

Finally, the suggested model is the steady-state. As such, neither the early stages of the arc development nor possible arc instabilities are described.

Acknowledgments

The authors wish to thank Yao-Wen Yeh and Jonathan Ng for their assistance with experiments and discussions. The authors also benefited from fruitful discussions of arc physics with Drs Mikhail Shneider, Igor Kaganovich and Michael Keidar. This work was supported by the U.S. Department of Energy, Office of Science, Basic Energy Sciences, Materials Sciences and Engineering Division.

References

[1] Fetterman A J, Raitses Y and Keidar M 2008 Enhanced ablation of small anodes in a carbon nanotube arc plasma *Carbon* **46** 1322–6

[2] Ng J and Raitses Y 2015 Self-organization processes in the carbon arc for nanosynthesis *J. Appl. Phys.* **117** 063303

[3] Shashurin A, Li J, Zhuang T, Keidar M and Beilis I I 2011 Application of electrostatic Langmuir probe to atmospheric arc plasmas producing nanostructures *Phys. Plasmas* **18** 073505

[4] Mesyats G A 2013 Ecton mechanism of the cathode spot phenomena in a vacuum arc *IEEE Trans. Plasma Sci.* **41** 676–94
[5] Shashurin A and Keidar M 2008 Factors affecting the size and deposition rate of the cathode deposit in an anodic arc used to produce carbon nanotubes *Carbon* **46** 1792–828
[6] Ostrogorsky A G and Marin C 2006 Heat transfer during production of carbon nanotubes by the electric-arc process *Heat Mass Transfer* **42** 470–7
[7] Keidar M and Beilis I I 2009 Modeling of atmospheric-pressure anodic carbon arc producing carbon nanotubes *J. Appl. Phys.* **106** 103304
[8] Tang D, Sun L, Zhou T, Zhou W and Xie S 2005 Two possible mechanisms involved in the arc discharge method of carbon nanotube preparation *Carbon* **43** 2812–6
[9] Alekseyev N I and Dyuzhev G A 2001 Arc discharge with a vaporizable anode: why is the fullerene formation process affected by the kind of buffer gas? *Tech. Phys.* **46** 1247–55
[10] Murphy A B 2010 The effect of metal vapor in arc welding *J. Phys. D: Appl. Phys.* **43** 434001
[11] Nemchinsky V A 2012 Cathode erosion in a high-pressure high-current arc: calculations for tungsten cathode in a free-burning argon arc *J. Phys. D: Appl. Phys.* **45** 135201
[12] Benilov M S 2008 Understanding and modeling plasma–electrode interaction in high-pressure arc discharges: a review *J. Phys. D: Appl. Phys.* **41** 144001
[13] Ng J and Raitses Y 2014 Role of the cathode deposit in the carbon arc for the synthesis of nanomaterials *Carbon* **77** 80–8
[14] Teste P H, Leblanc T, Rossignol J and Andlauer R 2008 Contribution to the assessment of the power balance at the electrodes of an electric arc in air *Plasma Sources Sci. Technol.* **17** 035001
[15] Null M R and Lozier W W 1958 Measurement of reflectance and emissivity of graphite at arc temperature with a carbon arc image furnace *J. Appl. Phys.* **29** 1605
[16] Anisimov S I 1968 Vaporization of metal absorbing laser radiation *Sov. Phys. JETP* **27** 182–3
[17] Ya Moizhes B and Nemchinsky V A 1980 Erosion and cathode jets in a vacuum arc *Sov. Phys. Tech.* **25** 438–41
[18] Nemchinsky V A 1982 Monte-Carlo calculation of the erosion rate and ion current at the vacuum arc cathode *Sov. Phys. Tech.* **27** 1073–7
[19] Benilov M S, Jacobsson S, Kaddani A and Zahrai S 2001 Vaporization of a solid surface in an ambient gas *J. Phys. D: Appl. Phys.* **34** 1993–9
[20] Keidar M, Fan J and Boyd I D 2001 Vaporization of heated materials into discharge plasmas *J. Appl. Phys.* **89** 3095–8
[21] www.iap.tuwein.ac.at/www/surface/vapor_pressure
[22] Joseph M, Sivakumar N and Manovari P 2004 Studies on equation of state of high temperature nuclear materials *Ann. Nucl. Energy* **31** 1163–75
[23] Powell R W and Schofield F H 1939 The thermal and electrical conductivities of carbon and graphite at high temperatures *Proc. Phys. Soc.* **51** 153–72